

Identification of the First Steps of the Electrochemical Polymerization of Pyrroles by Means of Fast Potential Step Techniques

Claude P. Andrieux, Pierre Audebert, Philippe Hapiot, and Jean-Michel Savéant*

Laboratoire d'Electrochimie Moléculaire de l'Université de Paris 7, Unité Associée au CNRS No. 438, 2 place Jussieu, 75251 Paris Cedex 05, France (Received: June 18, 1991)

The early stages of the electrochemical polymerization of three substituted pyrroles were investigated by means of fast double potential step chronoamperometry thanks to the use of electrodes in the micrometer diameter range. Systematic analysis of the reaction kinetics allowed the conclusion that, for all three pyrroles, the cation radicals, rather than the neutral radicals that would result from their deprotonation, are involved in the carbon-carbon bond forming process and that they couple between themselves rather than with the starting monomer.

Since its first synthesis by means of anodic electrochemical polymerization,^{1a} polypyrrole and substituted polypyrroles have been the subject of innumerable studies.^{1b} In spite of this intense activity, very little is known about the nature of the first steps of the polymerization process. Do they involve the monomer and oligomer cation radicals or the radicals resulting from their deprotonation? Does the carbon-carbon bond formation result from the coupling of radicals or from their reaction with the starting monomer? These queries have not received so far clear-cut answers mostly because the rapidity of these first steps has precluded their kinetic characterization at the benefit of latter stages of the reaction, particularly nucleation of the deposited polymer.² In a previous communication, we have shown that the use of ultramicroelectrodes³ (with diameters in the micrometer range) allows the observation of the cyclic voltammetric chemical reversibility of the primary redox at high scan rates in a series of substituted pyrroles.⁴ This opened a route to a more systematic investigation of the kinetics of the first steps of the polymerization process. The three substituted pyrroles shown in Figure 1 were selected for this purpose because the lifetime of their cation radicals is not too short,⁴ and therefore a detailed study of the mechanism in an extended range of measurement times was feasible. This is particularly true for TISPP, the cation radical of which has the longest lifetime in the series. Besides exploratory cyclic voltammetric experiments, the technique we used for quantitative analysis of the reaction mechanism was double potential step chronoam-

perometry which has the advantage that the current response provides kinetic information on the chemical steps that follow the initial electron transfer with negligible interference of the kinetics of the electron transfer, provided the electrode potential is stepped sufficiently beyond the potential where the oxidation wave appears. It is possible with this technique to use ultramicroelectrodes, thus allowing the investigation of a time window that has a fraction of a microsecond as lower limit.⁵ After the first potential step, the potential is stepped back to its initial value, at a time θ , which can be varied from one experiment to the other. The anodic current, $i(\theta)$, is measured at time θ and the cathodic current, $i(2\theta)$, at time 2θ . The ratio $i(2\theta)/i(\theta)$ is normalized toward the value $(i(2\theta)/i(\theta))_{\text{diff}}$ it would have in the absence of follow-up chemical steps so as to obtain the ratio^{5,6}

$$R = (i(2\theta)/i(\theta))/(i(2\theta)/i(\theta))_{\text{diff}}$$

The principle of the investigation consists in the determination of the variations of the current ratio R with the time θ , the concentration of the pyrrole monomer, and the addition of bases to the system.

All three pyrroles undergo electropolymerization upon electrolysis at a potential located beyond the wave of the monomer. While TISP and TISPP give rise to relatively thin polymer deposits, DMP produces a good quality polymer that has been shown to be slightly crystalline in contrast to polypyrrole itself.⁷

Results and Discussion

TISPP. Figure 2a shows typical cyclic voltammograms in the 20–100 V s⁻¹ range of scan rates when the system passes from almost complete irreversibility to complete reversibility. The variations of the ratio $i_p/v^{1/2}$ (i_p , anodic peak potential; v , scan rate), which is a measure of the apparent number of electrons passed during the oxidation process, are represented in Figure 2b.

The results of the double potential step experiments are shown in Figure 3. It is immediately apparent that the kinetics of the follow-up reactions, as measured by the current ratio R , are dependent upon the parameter $C^0\theta$ (C^0 is the concentration of the pyrrole in the bulk of the solution) in the sense that the same value of R is obtained by multiplying C^0 by any factor and simultaneously dividing θ by the same factor, and vice versa. This points to a second-order character of the kinetics of the set of reactions following the electron-transfer step.

On the other hand, the first important question to be answered concerning the reaction mechanism is to know whether the carbon-carbon bond formation involves the initially formed cation radical or the neutral radical resulting from its deprotonation:

(1) (a) Kanazawa, K. K.; Gardini, J. P.; Diaz, A. F. *J. Chem. Soc., Chem. Commun.* 1979, 635. (b) The literature on polypyrroles contains more than 1000 references. For a general review see ref 1c, and for a recent review on their electrocatalytic properties see ref 1d. (c) Street, G. B. *Handbook of Conducting Polymers*; Skotheim, T. A., Ed.; Marcel Dekker: New York, 1986; pp 265–291. (d) Deronzier, A.; Moutet, J. C. *Acc. Chem. Res.* 1989, 22, 249.

(2) (a) Genies, E. M.; Bidan, G.; Diaz, A. F. *J. Electroanal. Chem.* 1983, 149, 101. (b) Asavapiriyamont, S.; Chandler, G. K.; Gunwardena, G. A.; Pletcher, D. *J. Electroanal. Chem.* 1984, 177, 229. (c) Kim, K. J.; Song, H. S.; Kim, J. D.; Chon, J. K. *Bull. Korean Chem. Soc.* 1988, 9, 248. (d) Hillman, A. R.; Mallin, E. F. *J. Electroanal. Chem.* 1987, 220, 351. (e) Beck, F.; Oberst, M.; Jansen, R. *Electrochim. Acta* 1990, 35, 1841. (f) Shishiri, T.; Toriumi, M.; Tanaka, K.; Yamabe, T. *Synth. Met.* 1989, 33, 389. (g) Tanaka, K.; Shishiri, T.; Toriumi, M.; Yamabe, T. *Synth. Met.* 1989, 30, 271. (h) The situation is similar in the case of polythiophenes.²⁴ (i) Lang, P.; Chao, F.; Costa, M.; Garnier, F. *Polymer* 1987, 28, 668. (j) Downard, A. J.; Pletcher, D. *J. Electroanal. Chem.* 1986, 206, 147. (k) Lang, P.; Chao, F.; Costa, M.; Garnier, F. *J. Chim. Phys.* 1989, 86, 107. (l) Tourillon, G. *Handbook of Conducting Polymers*; Skotheim, T. A., Ed.; Marcel Dekker: New York, 1986; pp 293–350. (m) It is also noteworthy that there are only few examples of systematic analysis of the kinetics of oxidative dimerizations and that no general rules seem to emerge as to the nature of the coupling step: it is of the cation radical type in some instances²⁵ and of the cation radical-cation radical type in others.^{26p} (n) Amatore, C.; Savéant, J.-M. *J. Electroanal. Chem.* 1983, 144, 59. (o) Yang, H.; Bard, A. J. *J. Electroanal. Chem.*, in press. (p) Larumbe, D.; Gallardo, I.; Andrieux, C. P. *J. Electroanal. Chem.*, in press.

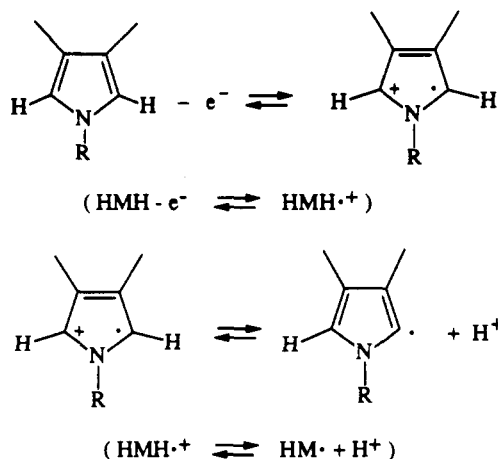
(3) Andrieux, D. P.; Hapiot, P.; Savéant, J.-M. *Chem. Rev.* 1990, 90, 723.

(4) Andrieux, C. P.; Audebert, P.; Hapiot, P.; Savéant, J.-M. *J. Am. Chem. Soc.* 1990, 112, 2439.

(5) Andrieux, C. P.; Hapiot, P.; Savéant, J.-M. *J. Phys. Chem.* 1988, 92, 5992.

(6) Andrieux, C. P.; Savéant, J.-M. *Electrochemical Reactions. In Investigations of Rates and Mechanisms of Reactions*; Bernasconi, C. F., Ed.; Wiley: New York, 1986; Vol. 6, 4/E, Part 2, pp 305–390.

(7) Waltman, R. J.; Bargon J. *Tetrahedron* 1984, 40, 39.

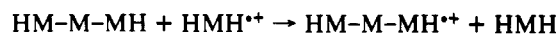
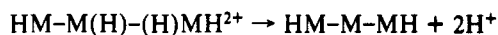
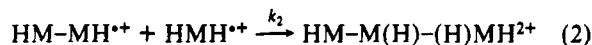
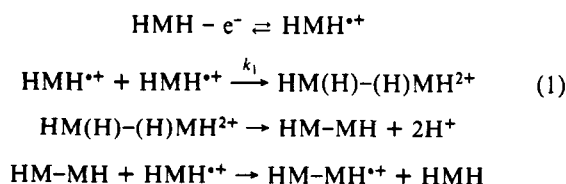


To answer this question, we carried out a cyclic voltammetric experiment with a concentration of pyrrole of 5 mM and with scan rates ranging between 200 and 2000 V s⁻¹, i.e., between irreversibility and reversibility, in which we added to the solution increasing amounts of 2,6-di-*tert*-butylpyridine up to a concentration of 100 mM. This particular base was selected because it is a poor nucleophile owing to the steric hindrance of the two ortho *tert*-butyl groups and is, at the same time, a much stronger base than acetonitrile used as the solvent (pK_a = 11.8 in acetonitrile).⁸ We found that the addition of the base had no noticeable effect on the voltammograms. This result, combined with the observed dependency of the double potential step data on C^{0θ}, unambiguously shows that the neutral radical, HM•, is not an intermediate on the reaction pathway. Indeed, if the deprotonation step were not rate determining but acting as a preequilibrium vis-à-vis a follow-up rate-determining step, the overall rate of the reaction should be increased by the addition of the base. In the case where the deprotonation step would be rate determining, the addition of the base should also accelerate the reaction unless the cation radical is so strong an acid that it would deprotonate spontaneously regardless of the presence of the base. In the latter situation, however, the double potential step response should be independent of C⁰ at variance with the experimental observations.

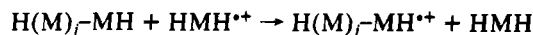
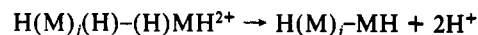
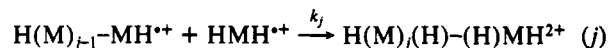
The conclusion that the neutral radical is not an intermediate in the carbon-carbon bond forming process falls in line with the results of a recent study of spin trapping of intermediates during the chemical oxidation of pyrrole.^{2f} The absence of spin trapping by nitrosobenzene and other spin traps was taken as an indication of the absence of the neutral σ-radical in the polymerization process. It should be noted however that this observation does not unambiguously prove the conclusion since the carbon-carbon bond forming reactions could be faster than the reaction with the spin trap.

Once the intermediacy of the cation radical rather than of the neutral radical in the carbon-carbon bond formation is established, the next problem to be solved is that of the nature of the bond formation process. Does it involve the coupling of two cation radicals (CR-CR) or the attack of one cation radical on the starting pyrrole (CR-S)?

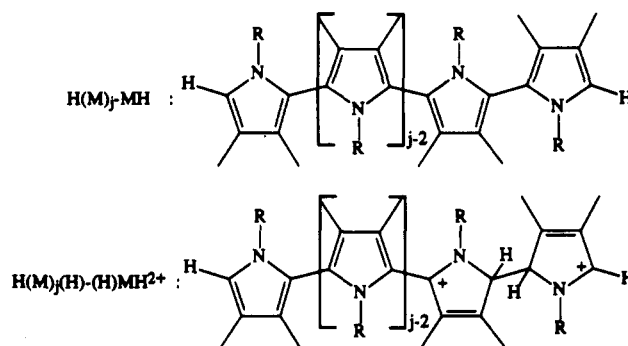
In the CR-CR case, we consider the following reaction scheme.



⋮



The notations are defined by the following equivalencies:



The reaction scheme above contains simplifications that require some justification. The coupling steps are represented as irreversible in the sense that the corresponding backward reactions are regarded as slower than the deprotonation that follows each of them. Evidence supporting this assumption is provided by the previous observation that the addition of a base does not affect the kinetics of the overall reaction. It also falls in line with the fact that pyrrole itself is a very poor base⁹ and that, in the dication, each of the two pyrrole moieties that bear a positive charge resembles a protonated pyrrole. The formation of each oligomer has been represented as resulting from the coupling of the cation radical of the preceding oligomer and of that of the monomer. In fact, additional cation radical-cation radical coupling reactions may interfere. For example, the tetramer dication could result from the coupling of two dimer cation radicals as well as from that of the trimer and monomer cation radicals, the pentamer dication could result from the coupling of the trimer and dimer cation radicals as well as from that of the tetramer and monomer cation radicals, and so forth. As made clear in the following, the presence of these additional possible coupling steps would not significantly affect the shape of the relationship between the current ratio *R* and the parameter C^{0θ}.

Oxidation of the oligomers, H(M)_j-MH, by the cation radical of the monomer, HMH•+, is regarded as fast and irreversible in view of the fact that oligomers of pyrrole have been shown to be much easier to oxidize than pyrrole itself,¹⁰ as expected from the conjugation between the various monomeric units that exists in such compounds. The oxidation of each oligomer, H(M)_j-MH, starting with the dimer, could in principle take place at the electrode surface rather than occur in the solution from electron transfer to the cation radical of the monomer. However, on the time scale of the experiments, the formation of any of the oligomers is not very fast since the system is not far from reversibility and, thus, the solution oxidation overruns the electrode oxidation.^{6,11}

(8) (a) Schlesener, C. J.; Amatore, C.; Kochi, J. K. *J. Am. Chem. Soc.* **1984**, *106*, 7472 and references therein. (b) It might be argued that, although thermodynamically strong enough, the base could be kinetically ineffective because of steric hindrance. In fact, this base gives rise to quite fast deprotonation reactions even though slower (by 1–2 orders of magnitude) than with unencumbered bases of similar pK_a's, as shown previously in the deprotonation of alkylbenzene cation radicals.^{8a}

(9) Jones, R. A.; Bean, B. P. *The Chemistry of Pyrroles, Organic Chemistry, A Series of Monographs*; Blomquist, A. T., Wasserman, H. H., Eds.; Academic Press: New York, 1977; Vol. 34, pp 11–50.

(10) (a) Diaz, A. F.; Crowley, J.; Bargon, J.; Gardini, G. P.; Torrance, J. B. *J. Electroanal. Chem.* **1981**, *121*, 355. (b) Bredas, J. L.; Silbey, R.; Boudreaux, D. S.; Chance, R. R. *J. Am. Chem. Soc.* **1983**, *105*, 6555.

(11) (a) Amatore, C.; Savéant, J.-M. *J. Electroanal. Chem.* **1978**, *86*, 227. (b) Amatore, C.; Gareil, M.; Savéant, J.-M. *J. Electroanal. Chem.* **1984**, *176*, 377.

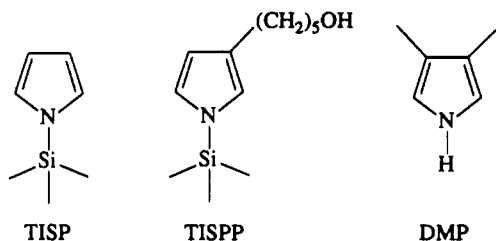


Figure 1. Substituted pyrroles investigated in this work with their conventional designations.

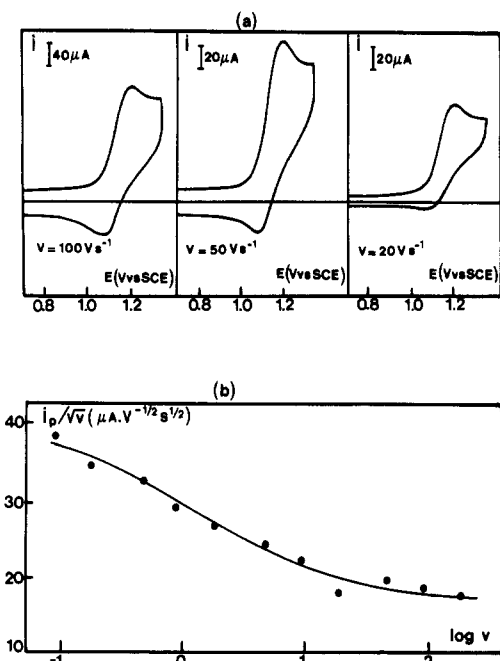
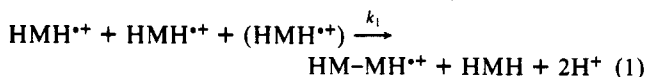
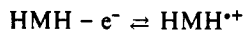
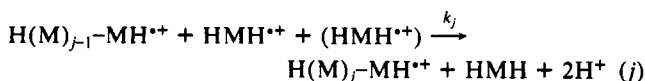


Figure 2. Cyclic voltammetry of TISPP (2 mM) in acetonitrile + 0.6 M NEt_4ClO_4 on a 1-mm-diameter platinum disk working electrode at 20 °C: (a) typical voltammograms; (b) variation of $i_p/v^{1/2}$ (i_p = anodic peak potential, v = scan rate) with the scan rate.

It follows from the preceding remarks that the oligomers, $\text{H(M)}_j\text{-MH}$, and their dication, $\text{H(M)}_j(\text{H})\text{-(H)MH}^{2+}$, do not accumulate in the solution; i.e., their concentrations obey the steady-state assumption. The above reaction scheme can thus be further simplified so as to become



⋮



(Each molecule of HMH^{*+} in parentheses in the left-hand members of the above equations does not participate in rate determination but merely completes the stoichiometry.)

The next question is that of the comparison between the rate constants of the successive coupling steps, $k_1, k_2, k_3, \dots, k_j$. Two extreme situations can be envisaged: one in which the first coupling step, leading to the dimer, is much faster than all the successive ones and, conversely, another one in which the first coupling step is much slower than all the others.

In the first case, as shown in the Appendix, the number of electrons per molecule passes from 1 to 1.5 as the dimerization reaction becomes faster and faster, i.e., as one passes from complete

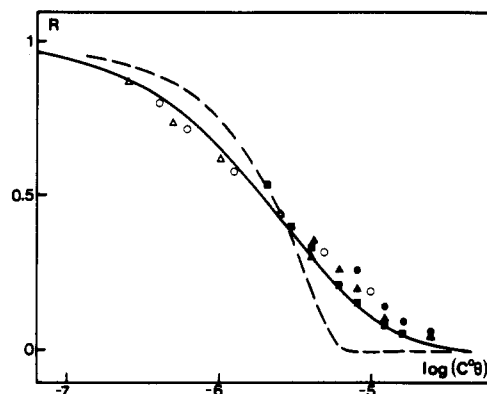


Figure 3. Double potential step (from 0.7 to 1.45 Vvs SCE and back) chronoamperometry of TISPP in acetonitrile + 0.6 M NEt_4ClO_4 . Variation of the ratio R with the parameter $C^0\theta$, on a 1 mm ($\bullet, \blacktriangle, \blacksquare$) and a 20 μm (\circ, \triangle) diameter platinum disk for different values of C^0 ; (Δ) 10 mM, (\bullet, \circ) 4 mM, ($\blacktriangle, \blacksquare$) 2 mM, (\blacksquare) 1 mM. Full line: working curve for a CR-CR mechanism. Dashed line: working curve for a CR-S-irr mechanism.

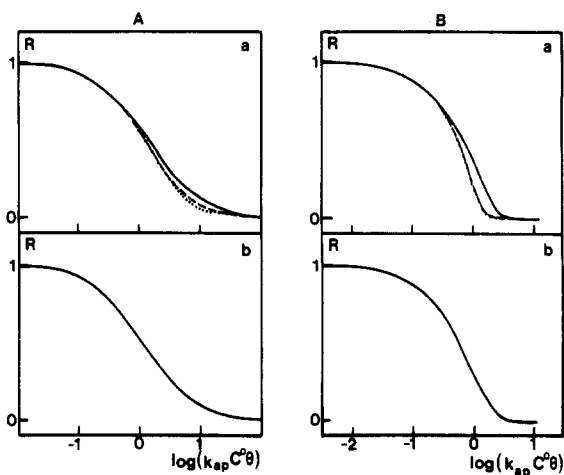


Figure 4. Working curves relating the current ratio R to the dimensionless kinetic parameter $k_{ap}C^0\theta$. (A) Cation radical-cation radical coupling mechanism. (a) full line: $k_1 \neq 0, k_2 = k_3 = k_4 = \dots = k_j \dots = 0$, dashed line: $k_1 = k_2 \neq 0, k_3 = k_4 = \dots = k_j \dots = 0$; dotted line: $k_1 = k_2 = k_3 \neq 0, k_4 = \dots = k_j \dots = 0; k_{ap} = 3k_1$. (b) $k_1 \ll k_2, k_3, k_4, \dots, k_j, \dots; k_{ap} = 2nk_1$ ($n \rightarrow \infty$). (B) Cation radical-substrate irreversible coupling mechanisms ($k_1' \gg k_{-1}, k_2' \gg k_{-2}, k_3' \gg k_{-3}, k_4' \gg k_{-4}, \dots, k_j' \gg k_{-j}, \dots$). (a) full line: $k_1' \neq 0, k_2' = k_3' = k_4' = \dots = k_j' \dots = 0$; dashed line: $k_1' = k_2' \neq 0, k_3' = k_4' = \dots = k_j' \dots = 0; k_{ap} = 3k_1'$. (b) $k_1' \ll k_2', k_3', k_4', \dots, k_j', \dots; k_{ap} = 2nk_1'$ ($n \rightarrow \infty$).

reversibility to complete irreversibility. The current ratio R is a function of the single dimensionless parameter $k_{ap}C^0\theta$, where k_{ap} is conveniently defined as $k_{ap} = 3k_1$, for normalization purposes that will appear in the following. The variation of R with $k_{ap}C^0\theta$ has the shape shown in Figure 4Aa.

In the second case, the steady-state assumption can be applied to all the oligomer cation radicals but the dimer and the last one ($j = n$) in the series. The exact value of n would depend on termination steps in the polymerization process. If n is large, the number of electrons per molecule tends to pass from 1 to 2^{12} as the dimerization reaction becomes faster and faster, i.e., as one passes from complete reversibility to complete irreversibility. The current ratio R is again a function of the single dimensionless parameter $k_{ap}C^0\theta$, where k_{ap} is defined as $k_{ap} = (2n + 1)k_1$. The variation of R with $k_{ap}C^0\theta$ has the shape shown in Figure 4Ab (see Appendix). We note that the shape of the R - $k_{ap}C^0\theta$ curve,

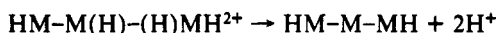
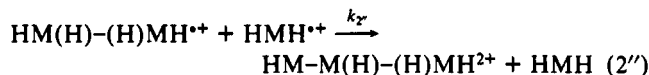
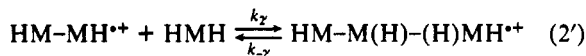
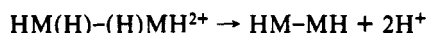
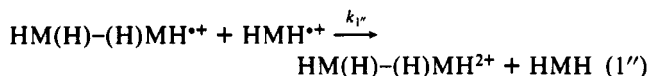
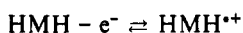
(12) In fact, when the number of monomer units is large, the polymer is, at the potential where the experiments are carried out, further oxidized so as to contain one positive charge for each ensemble of four polymer units.^{1c} The total number of electrons per molecule of starting monomer will thus tend toward 2.25 rather than toward 2.

although not identical, is quite similar to that in the first. They would be practically impossible to distinguish one from the other within experimental uncertainty.

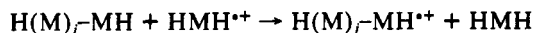
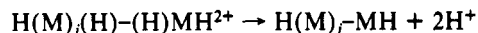
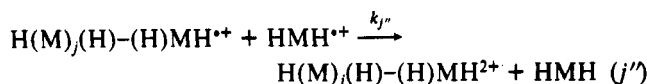
In fact, neither of these two extreme assumptions seems chemically reasonable. As j increases, starting from $j = 1$, i.e., from the coupling of two monomer cation radicals, the Coulombic repulsion that opposes the carbon-carbon bond formation decreases owing to the more and more extended delocalization of the charge in the $H(M)_j\text{-MH}^{2+}$ cation radical. This factor would thus lead to an acceleration of the coupling as the degree of oligomerization increases. There is however an opposite effect of the increase of electronic delocalization in the $H(M)_j\text{-MH}^{2+}$ cation radical. In the carbon-carbon bond forming process, we start with two sp_2 carbons that are converted into sp_3 carbons upon reaction. The attending nuclear reorganization in the $H(M)_j\text{-MH}^{2+}$ cation radical is the more severe, and therefore the reaction is the slower, the larger the extent of the electronic delocalization, i.e., the larger j . If we assume that these two opposite factors approximately compensate each other, i.e., that $k_1 = k_2 = k_3 = \dots k_j = \dots$, the following kinetic characteristics are obtained. (See Appendix for a mathematical and numerical analysis of the problem.) As seen in Figure 4Aa, the $R-k_{ap}C^0\theta$ curve obtained for the case where the process is stopped at the level of the trimer cation radical ($k_1 = k_2, k_3 = \dots k_j = \dots = 0$) is close to that of the first case above, when the process was stopped at the level of the dimer cation radical. If we go to the tetramer, there is even less variation of the $R-k_{ap}C^0\theta$ curve, and we then practically obtain the limiting curve corresponding to high values of j . This rapid convergence¹³ of the $R-k_{ap}C^0\theta$ curves toward a limiting behavior is a consequence of the fact that the concentration of the oligomer cation radical, $H(M)_j\text{-MH}^{2+}$, rapidly decreases as j increases.

The most important outcome of the above discussion is that the $R-k_{ap}C^0\theta$ curves characterizing the CR-CR case have very similar shapes whatever the relative magnitudes of the rate constants of the formation of the successive oligomer cation radicals may be. This also has as a consequence that the possible occurrence, that we have evoked earlier, of coupling between oligomer cation radicals besides coupling of oligomer cation radicals with the monomer cation radical would not significantly modify the shape of the $R-k_{ap}C^0\theta$ curve.

In the CR-S case, we consider the following reaction scheme:

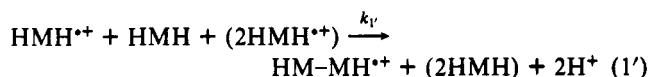
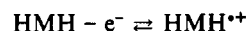


⋮

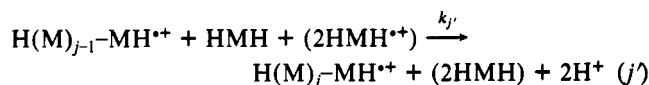


The formation of the oligomer dication, starting with the dimer dication, $H(M)_j\text{(H)-(H)MH}^{2+}$, involves a two-step process. We thus distinguish two limiting subcases. One will be denoted CR-S-irr, in which the coupling step is rate determining ($k_1 \gg k_{-1}, k_2 \gg k_{-2}, k_3 \gg k_{-3}, k_j \gg k_{-j}, \dots$), and the other denoted CR-S-rev, in which the coupling step acts as a preequilibrium vis-à-vis the following rate-determining electron-transfer step ($k_1 \ll k_{-1}, k_2 \ll k_{-2}, k_3 \ll k_{-3}, k_j \ll k_{-j}, \dots$). In both cases, the reactions following these first two steps are fast and irreversible as already discussed in the CR-CR case.

In the CR-S-irr subcase, it follows that the reaction scheme can be simplified as depicted below.

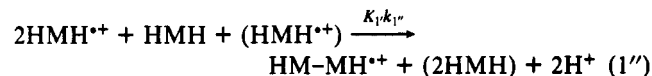
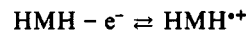


⋮

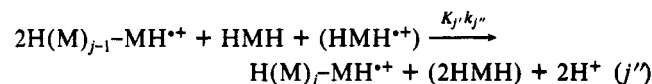


The current ratio R is a function of the parameter $C^0\theta$ as in the CR-CR case. The comparison between the rate constants of the successive coupling steps can be made in the same fashion as in the CR-CR case, resulting in the three versions of the $R-k_{ap}C^0\theta$ curve shown in Figure 4Ba,b. As before, we note that the shapes of the curves are very similar in all situations. We also note that this common shape is clearly different from that found in the CR-CR case, which makes the distinction between the two types of coupling mechanisms possible in spite of the fact that the structure of the kinetic parameter is the same with both mechanisms.

In the CR-S-rev subcase, for the same reasons as above, the reaction scheme can be simplified as follows.



⋮



Since the rate-determining step is second order in HMH^{2+} and first order in HMH , the kinetic parameter is now proportional to $C^0\theta$ instead of $C^0\theta$, which allows an easy distinction between the present mechanism and the CR-CR and CR-S-irr mechanisms. Following the same method as in the two preceding cases, the $R-k_{ap}C^0\theta$ curves shown in Figure 5a,b are obtained (see Appendix).

We can now analyze the double potential step data obtained with TISPP according to the various mechanistic possibilities just discussed. As noted before, the current ratio R is a function of the parameter $C^0\theta$ (Figure 3) which accords with either the CR-CR or the CR-S-irr mechanisms. To show unambiguously that

(13) In the analysis given in the Appendix, the diffusion coefficients of all oligomeric species are taken, for simplicity, as equal to one another and to that of the monomeric species. They in fact decrease when j increases, and thus the convergence is actually even more rapid than that reported in Figure 4Aa.

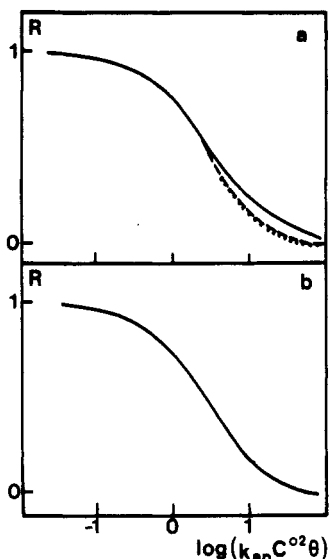


Figure 5. Working curves relating the current ratio R to the dimensionless kinetic parameter $k_{ap}C^{0.2\theta}$ for the cation radical-substrate reversible coupling mechanism ($k_{1'} \ll k_{-1'}$, $k_{2'} \ll k_{-2'}$, $k_{3'} \ll k_{-3'}$, ... $k_{p'} \ll k_{-p'}$...). (a) full line: $K_1 k_{1'} \neq 0$, $K_2 k_{2'} = K_3 k_{3'} = K_4 k_{4'} = \dots = K_p k_{p'} \dots = 0$; dashed line: $K_1 k_{1'} = K_2 k_{2'} \neq 0$, $K_3 k_{3'} = K_4 k_{4'} = \dots = K_p k_{p'} \dots = 0$; dotted line: $K_1 k_{1'} = K_2 k_{2'} = K_3 k_{3'} \neq 0$, $K_4 k_{4'} = \dots = K_p k_{p'} \dots = 0$, $k_{ap} = 3 K_1 k_{1'}$. (b) $K_1 k_{1'} < K_2 k_{2'}$, $K_3 k_{3'}$, $K_4 k_{4'}$, ... $K_p k_{p'}$, ..., $k_{ap} = 2n K_1 k_{1'}$ ($n \rightarrow \infty$).

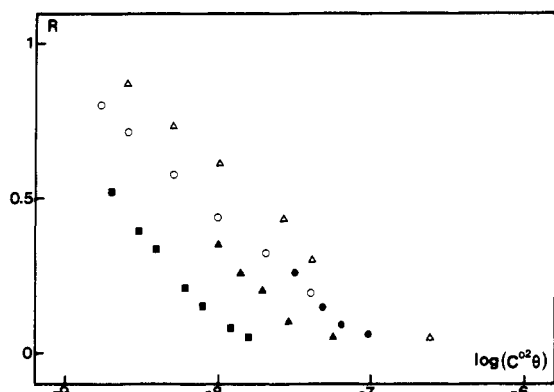


Figure 6. Double potential step (from 0.7 to 1.45 V vs SCE and back) chronoamperometry of TISPP in acetonitrile + 0.6 M NEt_4ClO_4 . Plot of the current ratio R against the parameter $C^{0.2\theta}$, on a 1 mm (\bullet , \blacktriangle , \blacksquare) and a 20 μm (\circ , \triangle) diameter platinum disk for different values of C^0 (\triangle) 10 mM, (\bullet , \circ) 4 mM, (\blacktriangle) 2 mM, (\blacksquare) 1 mM.

R does not depend on $C^{0.2\theta}$ beyond experimental uncertainty, we have replotted the data of Figure 3 against $C^{0.2\theta}$ instead of $C^{0\theta}$ (Figure 6). It is clearly seen that there is no correlation between the values of R and the parameter $C^{0.2\theta}$, thus ruling out the possible occurrence of the CR-S-rev mechanism. On the other hand, examination of the data shown in Figure 3 shows unambiguously that they fit the $R-k_{ap}C^{0\theta}$ curve that characterizes a CR-CR mechanism and not that of a CR-S-irr mechanism.

We thus conclude that, in the first steps of the electropolymerization process, carbon-carbon bond formation occurs by coupling of cation radicals and not by reaction of cation radicals with the starting pyrrole. It also appears that, during the time scale of the double potential step experiments, the degree of oligomerization is quite low. For $R = 0.1$, i.e., at the upper edge of the time window when the polymerization process has reached its maximal extent, the amount of trimer formed is only 30% of the dimer and the tetramer 10% (see Appendix). It is the very fact that the degree of polymerization is low during the potential step experiments that allowed us to analyze the kinetics and identify the first steps of the reaction in a straightforward manner, avoiding the complications that would have appeared upon deposition of the polymer onto the electrode surface. The analysis of the potential step data by means of the CR-CR working curve (Figure

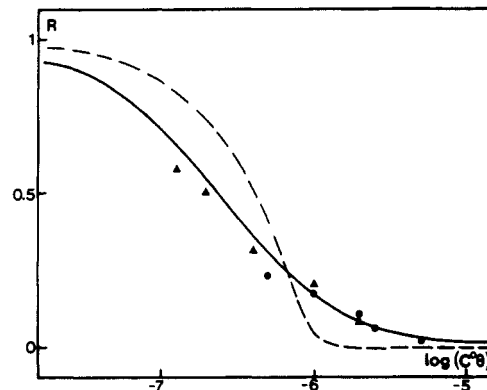


Figure 7. Double potential step (from 0.8 to 1.6 V vs SCE and back) chronoamperometry of TISP in acetonitrile + 0.6 M NEt_4BF_4 . Variation of the current ratio R with the parameter $C^{0\theta}$, on a 20 μm (\bullet , \blacktriangle) diameter platinum disk for different values of C^0 : (\bullet) 10 mM, (\blacktriangle) 4 mM. Full line: working curve for a CR-CR mechanism. Dashed line: working curve for a CR-S-irr mechanism.

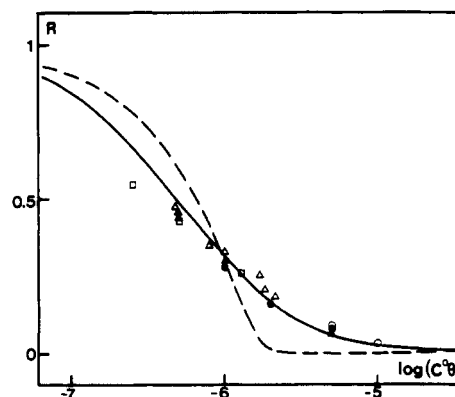


Figure 8. Double potential step (from 0.6 to 1.35 V vs SCE and back) chronoamperometry of DMP in acetonitrile + 0.6 M NEt_4ClO_4 . Variation of the ratio R with the parameter $C^{0\theta}$, on a 20 μm (\circ , \triangle , \square) and a 5 μm (\bullet , \blacktriangle) diameter platinum disk for different values of C^0 : (\circ , \bullet) 20 mM, (\triangle , \blacktriangle) 10 mM, (\square) 5 mM. Full line: working curve for a CR-CR mechanism. Dashed line: working curve for a CR-S-irr mechanism.

3) allows the determination of the rate constant of the rate-determining step: $k_1 = 2.2 \times 10^5 \text{ M}^{-1} \text{ s}^{-1}$. We also note that the number of electrons exchanged per molecule of pyrrole (2.2) found at low scan rate in cyclic voltammetry (Figure 2), when the polymerization process has had time to develop, is close to the expected value of 2.25 for a charged polymer.¹²

TISP. There is no obvious chemical reasons why the oxidative polymerization of TISP would follow a mechanism different from that of TISPP. This is indeed what we have found upon examination of the variations of the double potential step current ratio R with the parameter $C^{0\theta}$ (Figure 7). The rate constant of the formation of the dimer dication was found to be $k_1 = 1.8 \times 10^6 \text{ M}^{-1} \text{ s}^{-1}$.

DMP. This pyrrole might have different properties from the two others because of the two methyl substituents on the ring and of the H on the nitrogen. We have first checked that the current response is not affected by the addition of a base, showing that the carbon-carbon bond forming process involves cation radicals and not neutral radicals. As in the case of TISPP, 2,6-di-*tert*-butylpyridine was used as a base. Between 500 and 5000 V s^{-1} , i.e., between irreversibility and reversibility, we found no noticeable effect on the current response of the addition of the base up to 100 mM (with a concentration of pyrrole of 1 mM).

On the other hand, the double potential step current ratio R was again found to vary with $C^{0\theta}$ rather than with $C^{0.2\theta}$ (Figure 8) and to fit with the working curve characterizing a CR-CR mechanism and not that of a CR-S-irr mechanism. The electropolymerization of DMP thus appears to follow the same carbon-carbon bond forming mechanism as the other two pyrroles.

The rate constant of the dimerization of the monomer cation radicals was found to be $k_1 = 8.3 \times 10^5 \text{ M}^{-1} \text{ s}^{-1}$.

Experimental Section

Chemicals. TISP was prepared by condensation of triisopropylsilyl chloride with potassium pyrrolide. The syntheses of TISPP and DMP were performed according to published procedures.^{14a,b} In all experiments, the supporting electrolyte was tetraethylammonium perchlorate. It was recrystallized before use from a mixture of dry acetonitrile and dry diethyl oxide.

Electrodes and Instrumentation. *Experiments with Micrometric Electrodes.* The ultramicroelectrodes were prepared by sealing platinum wires (Goodfellow Metal Ltd.) in a capillary glass tube according to a previously described procedure.^{15a} The electrode was polished with 0.25- μm alumina paste. The reference electrode was an aqueous SCE and the counter electrode a platinum wire. The cell was placed in a Faraday cage. The potentiostat with a three-electrode configuration was the same as previously described.^{15a} The voltammograms and the chronoamperograms were recorded on a Nicolet 4094C/4080 digital oscilloscope (8 bits, 5-ns minimum sampling time). The function generator was an Enertec 4431. In the double potential step experiments, the current-time curves were repeated and accumulated four times, and the data were transferred into an IBM PC-AT computer for calculation of R^5 . The electrode was cleaned with paper between each determination of R . These were repeated at least 10 times, and the resulting values of R were averaged. Under these conditions, the reproducibility of the R measurements was found to be better than 0.05.

Experiments with Millimetric Electrodes. The working electrode was a 1-mm-diameter platinum disk polished with a 1- μm diamond paste before use. A home-built potentiostat equipped with positive feedback compensation^{15b} was used for the potential step experiments together with a PAR 175 Universal Programmer function generator. The current was recorded by means of a home-built acquisition device controlled by an Apple II micro-computer.

In all cases the temperature was 20 °C.

Conclusion

The main conclusion of this study is, for all three pyrroles investigated, that the cation radicals, rather than the neutral radicals that would result from their deprotonation, are involved in the carbon-carbon bond forming process and that they couple between themselves rather than with the starting monomer. In view of the structure of these three particular substituted pyrroles, there is no obvious chemical reason why pyrrole itself should not react in the same fashion although its proper study is precluded for the moment by the too large reactivity of its cation radical.

Appendix

The $R-k_{\text{ap}}C^0\theta$ curves characterizing each of the three mechanisms were obtained by numerical computation, according to the Schmidt method,¹⁶ of the three sets of partial derivative equations, initial and boundary conditions below, using the following dimensionless variables: $\tau = t/\theta$ (t = time; θ = time at which the potential step is inverted); $y = x/(D\theta)^{1/2}$ (the diffusion is linear; x = distance from the electrode; D = diffusion coefficient, assumed to be the same for all intervening species¹³); $a_0 = [\text{HMH}]/C^0$, $a_1 = [\text{HMH}^+]/C^0$, $a_2 = [\text{HM-MH}^+]/C^0$, ..., $a_j = [\text{H}(\text{M})_{j-1}^-\text{MH}^+]/C^0$, ..., $\lambda_1 = k_1C^0\theta$, $k_1C^0\theta$, $K_1k_1C^0\theta$, $\lambda_2 = k_2C^0\theta$, $k_2C^0\theta$,

$K_2k_2C^0\theta$, ..., $\lambda_j = k_jC^0\theta$, $k_jC^0\theta$, $K_jk_jC^0\theta$, ..., (C^0 = bulk concentration of the monomer).

CR-CR

$$\frac{\partial a_0}{\partial \tau} = \frac{\partial^2 a_0}{\partial y^2} + \lambda_1 a_1^2 + \lambda_2 a_1 a_2 + \dots + \lambda_j a_1 a_j + \dots$$

$$\frac{\partial a_1}{\partial \tau} = \frac{\partial^2 a_1}{\partial y^2} - 3\lambda_1 a_1^2 - 2\lambda_2 a_1 a_2 - \dots - 2\lambda_j a_1 a_j - \dots$$

$$\frac{\partial a_2}{\partial \tau} = \frac{\partial^2 a_2}{\partial y^2} + \lambda_1 a_1^2 - \lambda_2 a_1 a_2$$

⋮

$$\frac{\partial a_j}{\partial \tau} = \frac{\partial^2 a_j}{\partial y^2} + \lambda_{j-1} a_1 a_{j-1} - \lambda_j a_1 a_j$$

⋮

CR-S-irr

$$\frac{\partial a_0}{\partial \tau} = \frac{\partial^2 a_0}{\partial y^2} + \lambda_1 a_0 a_1 + \lambda_2 a_0 a_2 + \dots + \lambda_j a_0 a_j + \dots$$

$$\frac{\partial a_1}{\partial \tau} = \frac{\partial^2 a_1}{\partial y^2} - 3\lambda_1 a_0 a_1 - 2\lambda_2 a_0 a_2 - \dots - 2\lambda_j a_0 a_j - \dots$$

$$\frac{\partial a_2}{\partial \tau} = \frac{\partial^2 a_2}{\partial y^2} + \lambda_1 a_0 a_1 - \lambda_2 a_0 a_2$$

⋮

$$\frac{\partial a_j}{\partial \tau} = \frac{\partial^2 a_j}{\partial y^2} + \lambda_{j-1} a_0 a_{j-1} - \lambda_j a_0 a_j$$

⋮

CR-S-rev

$$\frac{\partial a_0}{\partial \tau} = \frac{\partial^2 a_0}{\partial y^2} + \lambda_1 a_0 a_1^2 + \lambda_2 a_0 a_1 a_2 + \dots + \lambda_j a_0 a_1 a_j + \dots$$

$$\frac{\partial a_1}{\partial \tau} = \frac{\partial^2 a_1}{\partial y^2} - 3\lambda_1 a_0 a_1^2 - 2\lambda_2 a_0 a_1 a_2 - \dots - 2\lambda_j a_0 a_1 a_j - \dots$$

$$\frac{\partial a_2}{\partial \tau} = \frac{\partial^2 a_2}{\partial y^2} + \lambda_1 a_0 a_1^2 - \lambda_2 a_0 a_1 a_2$$

⋮

$$\frac{\partial a_j}{\partial \tau} = \frac{\partial^2 a_j}{\partial y^2} + \lambda_{j-1} a_0 a_1 a_{j-1} - \lambda_j a_0 a_1 a_j$$

⋮

$$\tau = 0, y \geq 0: \quad a_0 = 1, \quad a_1 = a_2 = \dots = a_j = 0$$

$$y = 0, \tau \geq 0: \quad \frac{\partial a_0}{\partial y} + \frac{\partial a_1}{\partial y} = 0, \quad \frac{\partial a_2}{\partial y} = \dots = \frac{\partial a_j}{\partial y} = \dots = 0$$

$$0 \leq \tau \leq \theta: \quad a_0 = 0 \quad \tau \geq \theta: \quad a_1 = 0$$

The current flowing through the electrode is given by

$$\frac{i}{FSC^0D^{1/2}} = \left[\frac{\partial a_0}{\partial y} \right]_{y=0}$$

and thus the ratio R can be obtained from

$$R = \left[\frac{\partial a_0}{\partial y} \right]_{y=0, \tau=2} / \left[\frac{\partial a_0}{\partial y} \right]_{y=0, \tau=1}$$

In all three cases, appropriate linear combination of the successive partial derivative equations leads, for a degree of polymerization $j = n$, to

(14) (a) Farnier, M.; Fournari, P. *Bull. Soc. Chim. Fr.* **1975**, 2335. (b) Andrieux, C. P.; Audebert, P.; Merz, A.; Schwarz, R. *New J. Chem.* **1990**, *14*, 637.

(15) (a) Andrieux, C. P.; Garreau, D.; Hapiot, P.; Pinson, J.; Savéant, J.-M. *J. Electroanal. Chem.* **1988**, *243*, 321. (b) Garreau, D.; Savéant, J.-M. *J. Electroanal. Chem.* **1972**, *35*, 309.

(16) Crank, J. *Mathematics of Diffusion*; Oxford University Press: London, 1956.

$$\frac{\partial[(2n+1)a_0 + na_1 + (n-1)a_2 + (n-2)a_3 + \dots + a_n]/\partial\tau = \partial^2[(2n+1)a_0 + na_1 + (n-1)a_2 + (n-2)a_3 + \dots + a_n]/\partial y^2}$$

Therefore, at any time

$$\frac{1}{\pi^{1/2}} \int_0^\tau (n+1) \frac{i(\eta)}{FSC^0 D^{1/2}} d\eta = (2n+1) - [(2n+1)a_0 + na_1 + (n-1)a_2 + (n-2)a_3 + \dots + a_n]_{y=0}$$

Thus, during the anodic potential step, the current varies between two limits corresponding to complete reversibility ($[a_0]_{y=0} = 0$, $[a_1]_{y=0} = 1$, $a_{j=2..n} = 0$):

$$\frac{i(t)}{FSC^0 D^{1/2}} = \frac{1}{(\pi t)^{1/2}}$$

and complete irreversibility ($[a_0]_{y=0} = 0$, $[a_{j=1..n}]_{y=0} = 0$):

$$\frac{i(t)}{FSC^0 D^{1/2}} = \frac{2n+1}{n+1} \frac{1}{(\pi t)^{1/2}}$$

In other words, the number of electrons per monomer passes from 1 to $(2n+1)/(n+1)$, i.e., to 2 when n is large (not taking account of the additional charging of the polymer¹²). The same is true in cyclic voltammetry.

Two types of calculations were performed for each mechanism. We first set all λ 's equal to zero except λ_1 , then all λ 's were made equal to zero except λ_1 and λ_2 , λ_2 was made equal to λ_1 , finally all λ 's were made equal to zero except λ_1 , λ_2 , and λ_3 , and λ_2 and λ_3 were made equal to λ_1 . The resulting $R-k_{ap}C^0\theta$ curves are represented in parts Aa and Ba of Figure 4 for the CR-CR and CR-S-irr mechanisms, respectively, while the resulting $R-k_{ap}C^0\theta^2$ curves are represented in Figure 5a for the CR-S-rev mechanism. The calculations could have been pursued for $\lambda_1 = \lambda_2 = \lambda_3 = \lambda_4$ and $(\lambda_j)_{j>4} = 0$ and so forth, but we noticed that the R curves

cease to vary appreciably in between the last two calculations (Figures 4Aa, Ba and 5a).

In the second series of calculations we apply the condition $\lambda_1 \ll (\lambda_j)_{j=2..n}$ and considered the case where $n \rightarrow \infty$. That amounts to replacing the preceding sets of partial derivative equations, initial and boundary conditions, by the following ones.

CR-CR

$$\frac{\partial a_0}{\partial \tau} = \frac{\partial^2 a_0}{\partial y^2} + n\lambda_1 a_1^2$$

$$\frac{\partial a_1}{\partial \tau} = \frac{\partial^2 a_1}{\partial y^2} - 2n\lambda_1 a_1^2$$

CR-S-irr

$$\frac{\partial a_0}{\partial \tau} = \frac{\partial^2 a_0}{\partial y^2} + n\lambda_1 a_0 a_1$$

$$\frac{\partial a_1}{\partial \tau} = \frac{\partial^2 a_1}{\partial y^2} - 2n\lambda_1 a_0 a_1$$

CR-S-rev

$$\frac{\partial a_0}{\partial \tau} = \frac{\partial^2 a_0}{\partial y^2} + n\lambda_1 a_0 a^2$$

$$\frac{\partial a_1}{\partial \tau} = \frac{\partial^2 a_1}{\partial y^2} - 2n\lambda_1 a_0 a_1^2$$

$$\tau = 0, y \geq 0: \quad a_0 = 1, \quad a_1 = 0$$

$$y = 0, \tau \geq 0: \quad \frac{\partial a_0}{\partial y} + \frac{\partial a_1}{\partial y} = 0$$

$$0 \leq \tau \leq \theta: \quad a_0 = 0 \quad \tau \geq \theta: \quad a_1 = 0$$

Calculation of Lag Time for Convective-Reactive Diffusion

Jenn-Shing Chen*

Department of Applied Chemistry, National Chiao Tung University, Hsin Chu, Taiwan, ROC

and Franz Rosenberger

Center for Microgravity and Materials Research, University of Alabama in Huntsville, Huntsville, Alabama 35899 (Received: July 15, 1991)

Closed form solutions for the steady-state permeability P and the lag time L of a linear diffusion system with concurrent convection and reaction were obtained by two methods. In the first method, we identify the singularity at $s = 0$ of the Laplace transform of the total amount of diffusant, $\hat{Q}(s)$, released into the receiver as representation of the asymptotic diffusion behavior. P and L are then obtained from the time-independent coefficients of an expansion of $\hat{Q}(s)$ about $s = 0$. In the second method, we transform the convective-reactive diffusion equation into a form that contains only first and second derivatives of the concentration distribution function. By comparison of the resulting equation with that for a heterogeneous diffusion system, relationships of the convection velocity and rate constant with the position-dependent partition coefficient in heterogeneous diffusion is found. Taking advantage of the known solutions for permeability and lag time in heterogeneous diffusion, the corresponding expressions for P and L in convective-reactive diffusion are then obtained by transcription. These methods have the advantage over earlier approaches in that solutions in an infinite form are avoided.

Introduction

Diffusion plays an important role in numerous processes, such as chemical reactions in condensed phases,¹ nucleation,^{2,3} nerve

impulse transmission,⁴ and colloid flocculation.⁵ In recent years some attention has been paid to the mathematical description of transient diffusion.⁶⁻⁸ This requires complete solutions to diffusion

(1) For a recent review, see: Hänggi, P.; Talkner, P.; Borkovec, M. *Rev. Mod. Phys.* 1990, 62, 251.

(2) Frisch, H. L.; Carter, C. C. *J. Chem. Phys.* 1971, 54, 4326.

(3) Kelton, K. F.; Greerand, A. L.; Thompson, C. V. *J. Chem. Phys.* 1983, 79, 6261.

(4) Dudel, J. *Excitation, its Conduction and Synaptic Transmission, in Biophysics*; Hoppe, W., et al. Eds.; Springer-Verlag: Berlin, 1983; Chapter 15-1.

(5) Vold, R. D.; Vold, M. J. *Colloid and Interface Chemistry*; Addison-Wesley: London, 1983.